Burst Mode Message Loss Effects On WAAS Availability

Richard Fuller, Todd Walter, Per Enge

Department of Aeronautics and Astronautics
Stanford University

ABSTRACT
The Wide Area Augmentation System (WAAS) is a GPS-based navigation aid currently under development by the Federal Aviation Administration (FAA). WAAS will provide corrections to aviation users for the GPS clock, its ephemeris, and for the delay in its signal as it passes through the ionosphere. These corrections will be broadcast to users throughout the United States via geostationary satellites. A master station that combines data from a continental network of reference GPS receivers will create these messages. The geostationary satellites serve both as wide-area differential GPS data links as well as additional ranging sources. The data message stream of WAAS enhances the accuracy and integrity of the GPS signal for aviation. Simultaneously, the satellite ranging-source increases the percentage of time that the precise signal is available. In this way, WAAS provides needed improvements in four metrics over the standard GPS signal: accuracy, integrity, availability, and continuity.
The WAAS Signal-In-Space (SIS) has a limited data message bandwidth of 250 bits-per-second. This data bandwidth was chosen to balance two concerns. First, the power of the signal must not be so strong as to jam GPS. Second, the signal must provide the minimum amount of information necessary to ensure adequate accuracy and integrity for aviation users over the entire geostationary satellite footprint. The required message loss is specified not to exceed a rate of 0.001 (one loss per one-thousand messages) to ensure adequate system continuity and availability. The WAAS message structure is not particularly sensitive to independent message losses below the specified rate. Groups of missed messages (burst-mode) can prove to be a challenge in maintaining a continuous WAAS solution. The effects of burst-mode losses on the quality of the WAAS solution is presented and a Markov model for the burst message loss is developed. This research shows that WAAS availability can be achieved even with a message loss rate up to of 0.005 (i.e., five times the specification) even in the presence of burst-mode outages. This proves that the specification will ensure availability despite having been derived for independent message loss as opposed to burst losses.
Flight tests were conducted in California and Alaska to establish actual message loss profiles for aircraft. These flight test results were modeled and used in conjunction with NSTB reference station data to establish availability of WAAS solutions for various locations in the US. This research demonstrates that the GEO satellite fulfills its goals of providing accuracy, integrity, availability and continuity.

INTRODUCTION
The WAAS message structure is not particularly sensitive to independent loss rates below 0.001 as specified in [1]. The results in this paper show that even groups of missed messages (burst-mode) can be tolerated provided that the total message loss rate does not exceed a rate of 0.005. Flight tests were conducted in California and Alaska to establish actual message loss profiles for aircraft. The flight data is used to develop a Markov model for the observed burst-mode errors. Using the model, the effects of burst-mode errors on the availability of the WAAS solution are analyzed. The flight test model is used in conjunction with the NSTB reference station data to establish availability of WAAS solutions for various locations in the US. This latter exercise studies the impact of the combined effects of aircraft orientation and flight maneuvers on availability over the entire WAAS coverage region without conducting extra flight operations.

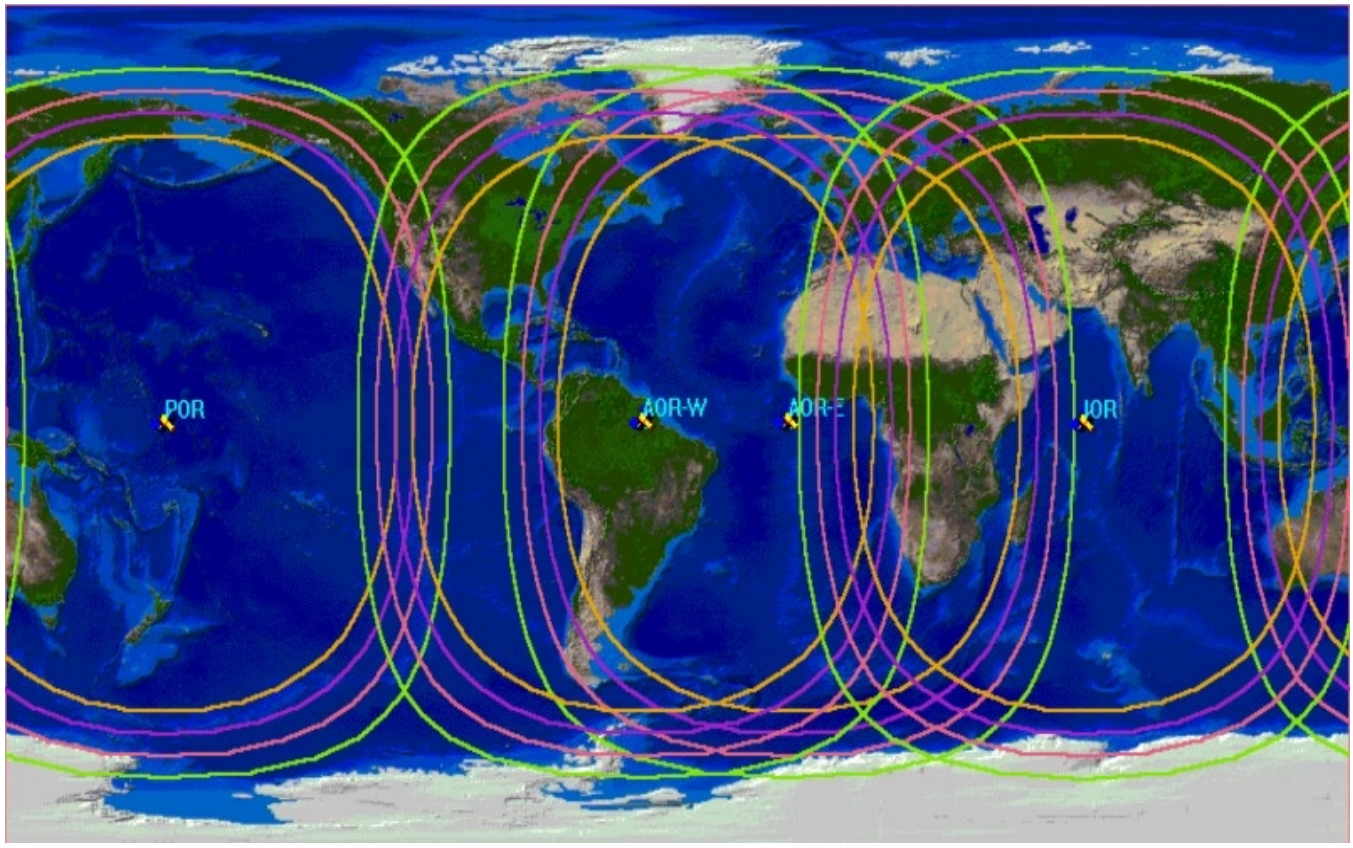

Figure 1: Geostationary Satellites Utilized for Satellite Based Augmentation Systems (WAAS and EGNOS). Contours of the User Elevations for 5, 10, 15, and 20 Degrees

OBSERVED MESSAGE LOSSES

The NovAtel MiLLenium receiver is a specially modified version with the capability to track a GEO signal and decode 250 bit messages with FEC encoding as described in [1]. The signal power levels measured by the receiver were collected along with the WAAS message packets. Figure 1 shows the four Inmarsat GEO satellites currently planned for two of the Space-Based Augmentation Systems: WAAS and the European Geostationary Navigation Overlay System (EGNOS). EGNOS is a system under development in Europe that will provide GPS and GLONASS corrections [2, 3]. Coordination of a standard wide-area correction message interface between WAAS and EGNOS will be overseen by the International Civil Aviation Organization (ICAO). This coordinated message structure has been published in [4].

EGNOS will be using Inmarsat's Atlantic Ocean Region-East (AOR-E) and Indian Ocean Region (IOR) satellites and WAAS is currently employing the Pacific Ocean Region (POR) and Atlantic Ocean Region-West (AOR-W) satellites. Both POR and AOR-W were used in this study. The contours represent the observation limits for users who employ 5, 10, 15 and 20 mask angles. The elevation of POR (PRN 134) at the Stanford University test location is about 15 degrees, while the elevation for AOR-W (PRN 122) is about 9 degrees.

During the period of the tests in October and November 1999, the GEO signals for both POR and AOR-W were often taken down to service the ground uplink system or to improve the messaging software. Many times the signal went down suddenly, without warning. For this reason, a test setup was required to differentiate between a lost message and a total absence of signal.

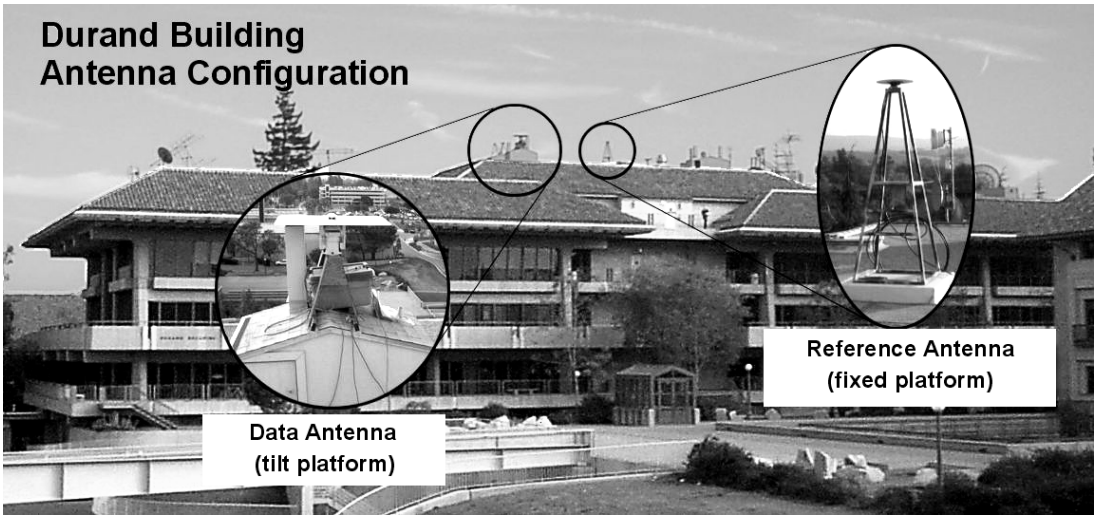

Figure 2: Rooftop Antenna Array Configuration

TEST SETUP AND EPOCH PROCESSING LOGIC

In order to make this differentiation, two identical receivers were used, comparing messages received at each epoch. Figure 2 shows the two antennas placed on top of the Durand Building at Stanford University. The fixed reference antenna is the same as that used by the NSTB site at Stanford. The antenna mounted on the tilt platform was used as the test receiver and had the capability to use the gain pattern of the antenna itself to vary the power of the incoming signal.

Figure 3 shows the logic design to process the two message streams. If the data receiver (connected to the tilt platform antenna) does not record a message at a given epoch and the reference receiver (fixed reference antenna) does record the message, then there must have been a signal available for processing and therefore this is counted as a lost message. If neither receiver collects a message then it is assumed that there was no message broadcast and the event is not included in the statistics. If the test receiver records a valid message, the signal is assumed to be present and the message is counted as received. This method was implemented to reject the cases when there were no messages being broadcast by the satellite.

If neither the data receiver nor the reference receiver records a message, then it is likely that the signal was not present at that epoch (a satellite outage). This can be justified by the combined probability of dual message losses between two separate receivers. The level of message loss required to meet the requirements for WAAS [1] is $\leq 10^{-3}$. Assuming that the message losses between the two receivers are independent [5, 6], then the chances of two receivers missing the same message is $\left(\leq 10^{-3}\right) \cdot \left(\leq 10^{-3}\right) \leq 10^{-6}$. The fraction of epochs ($\approx 10^{-6}$) that are potentially excluded will place an insignificantly small bias on the results.

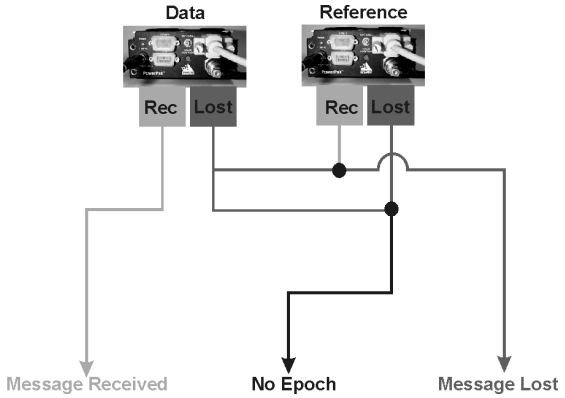

Figure 3: Epoch Processing Logic for GEO Messages

This method could have been used to track and capture messages for two GEOs simultaneously. However, there are processing limitations in the test receiver which made simultaneous tracking of the two GEOs difficult. It was apparent that the addition of a second GEO satellite to the tracking list of the receiver severely reduced the ability of both message streams to be decoded. The assumed reason for this problem was insufficient processing power in the receiver to compute the FEC decoding for two GEOs. Tracking of a single GEO satellite was observed to occupy as much as 15% of the receiver's CPU. The nominal margin without tracking any GEO satellites was about 20%. Flight test results that combined information from two GEO data streams were presented in [7]. Those results confirmed some degradation in the signal availability while tracking two GEO satellites.

OBSERVED MESSAGE LOSSES VERSUS SNR

The WAAS specification for loss rate was established to meet aviation availability requirements. Since messages

are repeated, a message loss rate of 10^{-3} represents a probability $10^{-3} * 10^{-3} = 10^{-6}$ for successive messages to be lost if the losses are independent. The chance of three successive losses is 10^{-9} for independent losses. Hence, the probability of three successive key messages being lost is less than the 10^{-8} integrity requirement. It will be shown in a later section of this paper that the assumption of message loss independence is not correct and that flight message losses tend to occur in bursts. This is different than the assumption in the previous section where the losses between two receivers are assumed independent. The burst mode errors are correlated in time for a single receiver.

The 32 dB-Hz threshold was established by [8] as a reasonable real-world limit for the minimum power level capable of achieving a 10^{-3} loss rate. The gray shaded region shown in the upper right-hand corner of Figure 4 represents the intersection of the 32 dB-Hz threshold and the 10^{-3} loss rate. No requirement is placed on a signal less than 32 dB-Hz; this is taken to be the minimum practical tracking level.

Using the method described in the previous section, 2.6 million data points were collected in the fall of 1999. The signal power levels measured by the receiver were collected along with the WAAS message packets. Slight adjustments in the angle on the tilt table were introduced to vary the power level going into the receiver. By tilting the antenna, power levels could be changed via the gain pattern.

The data was collected and grouped into bins that were 2 dB-Hz wide and the relative message losses for each bin are plotted in Figure 4. Also shown in Figure 4 are the theoretical and simulated results discussed in the previous section. The limiting region in the upper right-hand corner represents the specification for message loss given in [1]. The theoretical distribution presented in [9] had a 3 dB-Hz margin versus the specification. References [8] and [10] presented results that had very little or no margin with respect to the specification.

For comparison to the data collected here, the curve from [8] was chosen to nearly match the characteristics of the receiver used during the experiment. The error bars on each of the observed points are set at the width of the sampling interval in dB-Hz. The vertical extent error bars were determined from a Bernoulli distribution (the two-state case of the binomial distribution). The numbers below each observed point represent the number of samples taken in that bin.

The experimental data shows that the simulated, observed and specified levels are all approximately equal at 32 dB-Hz level. These results indicate that the message losses do meet the specification for the static receiver under these test conditions. However, there is very little or no margin for the receiver characteristics in question. At higher power levels, the loss rates are better than the specification.

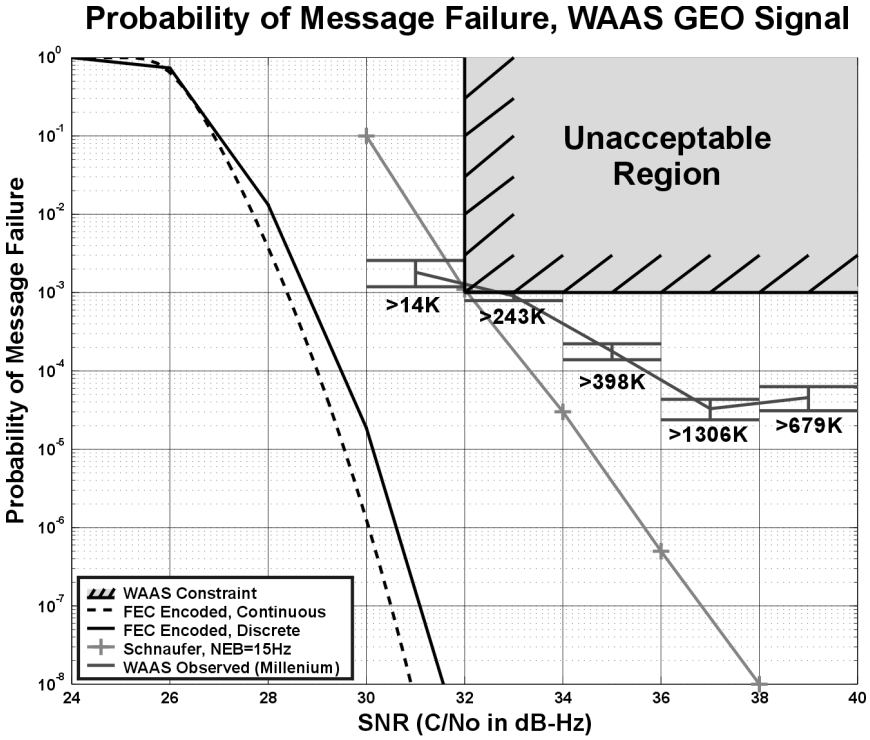

Figure 4: Static Station Message Loss Versus SNR

SNR FOR VARIOUS LOCATIONS ACROSS THE NSTB

To assess the significance of the low margin versus the specification, data were taken at a number of different locations across the US. These stations present a diversity of elevation angles to the GEO satellites. The station locations are shown in Figure 5. By measuring the received SNR values, comparison to the specified limit can be established.

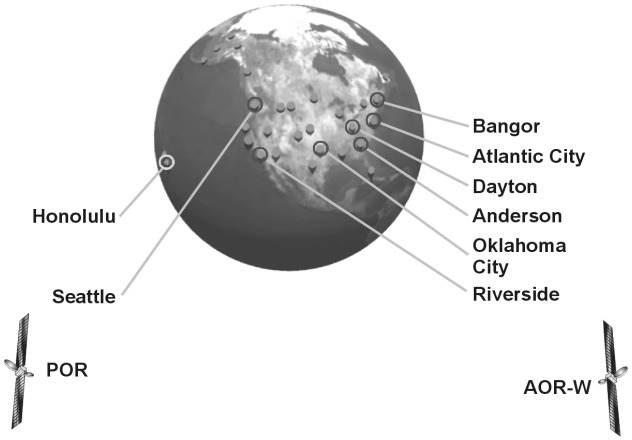

Figure 5: NSTB Locations Used with GEO Tracking

Figure 6 shows the SNR levels for eight stations located across the US. The majority of the stations in Figure 6 were tracking the satellite AOR-W or PRN 122. The labels for Honolulu and Seattle indicate the two stations were tracking POR or PRN 134. The expected trend of higher SNR for higher elevation is observed. The results from PRN 134 bound the highest and lowest elevations and fit the general trend of PRN 122.

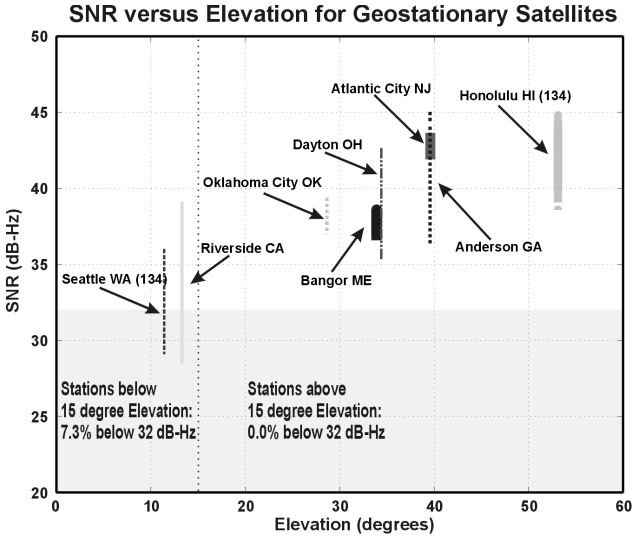

Figure 6: SNR Versus Elevation For Various Locations in the NSTB

For stations above a 15 degree elevation angle to the GEO, there were no recorded data points below 32 dB-Hz. For stations below a 15 degree elevation angle to the GEO, 7.3% of the points recorded below 32 dB-Hz. As shown in Figures 4 and 6 a user can expect to meet or exceed the specified message loss rate of 10^{-3} when the GEO satellite is in view above an elevation of 15 degrees. Below 15 degrees, the loss rate may not meet the specified level. The 7.3% of messages below 32 dB-Hz may have an impact on the availability of the WAAS solution for elevations between 10 and 15 degrees. While there is no data below 10 degrees of elevation, the trend in the data indicates that there may be a significant impact in message reception below 10 degrees.

The following section will examine the message loss results from flight tests. These flight tests were used as a basis for a Markov message loss model. This message loss model more accurately represents the burst-mode losses seen in flight as compared to independent losses assumed in previous work.

FLIGHT MESSAGE LOSSES

Over the course of June through December 1998 flight tests were conducted in Alaska and California to determine the message loss rate for an aircraft. Figure 7 shows the aircraft used in those flight tests. The aircraft used in the tests was equipped with multiple GPS-L1 antennas as well as a nose-mounted camera.

The GPS-L1 antennas served multiple purposes. Three GPS-based experiments were usually conducted in parallel: 1) attitude determination, 2) flight displays, and 3) WAAS navigation. Attitude determination experiments used differential carrier phase measurements from three or four GPS antennas to precisely determine the orientation of the aircraft [11]. The flight display research combined position and attitude information for presentation to the pilot. A representation of the data was projected on a small computer screen using 3D graphics to give the pilot increased situational awareness [12]. Figure 8 shows the system diagram for the flight test equipment used on the aircraft. The receiver was the same NovAtel MiLLenium™ as utilized in the first section. This test setup received the WAAS-compatible message stream broadcast by the Testbed Master Station (TMS) operating at Stanford University. This message stream was conveyed as shown in Figure 9. This figure shows the relay through network connection (ethernet) from Stanford to the FAA Technical Center in New Jersey. The Technical Center has the capability of routing the message stream to the uplink station in Santa Paula, California.

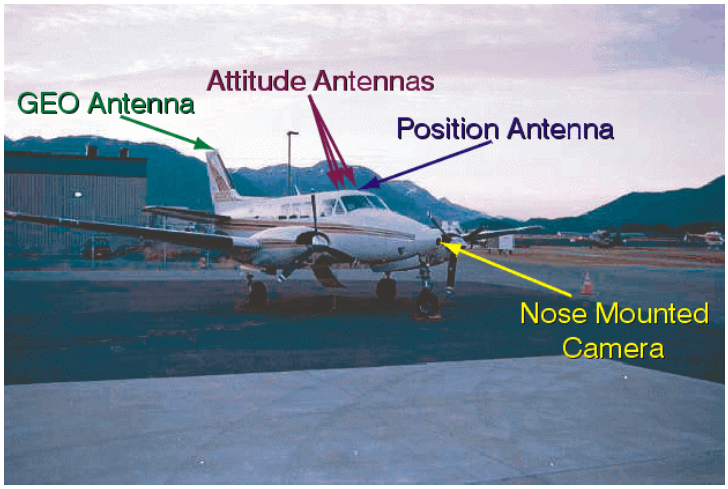

Figure 7: Flight Test Aircraft Used by Stanford University

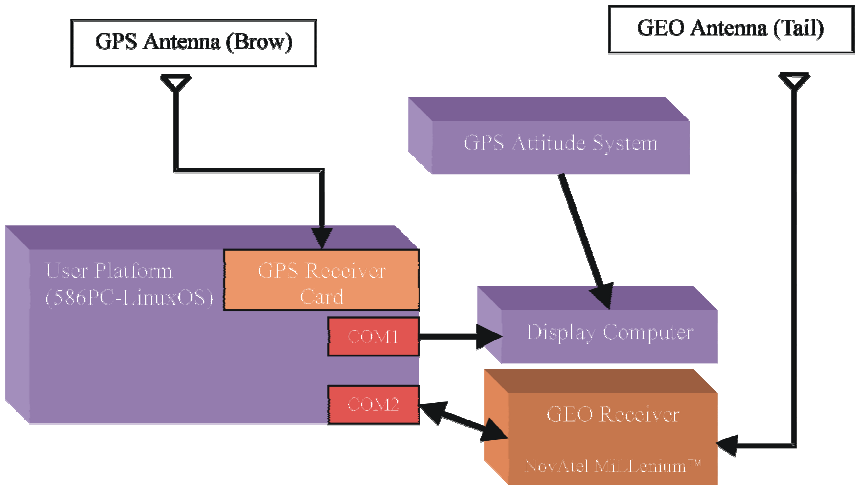

Figure 8: Flight Test System Diagram

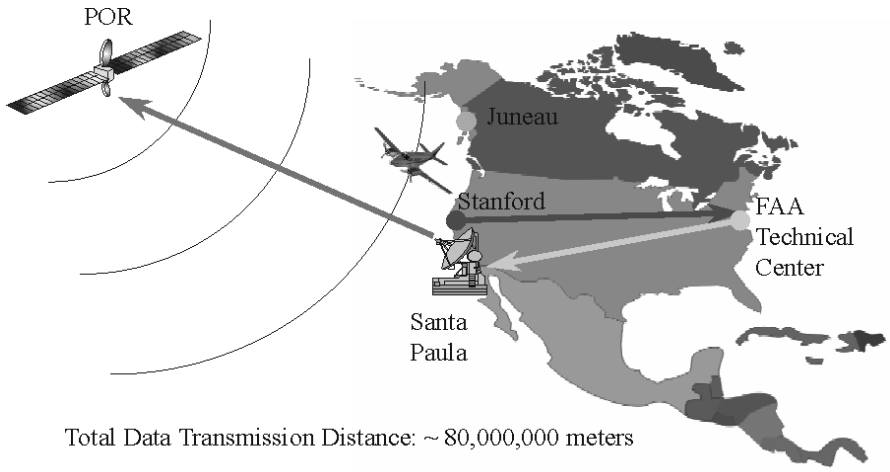

Figure 9: Flight Test Data Link. Test Bed Master Station Located at Stanford University

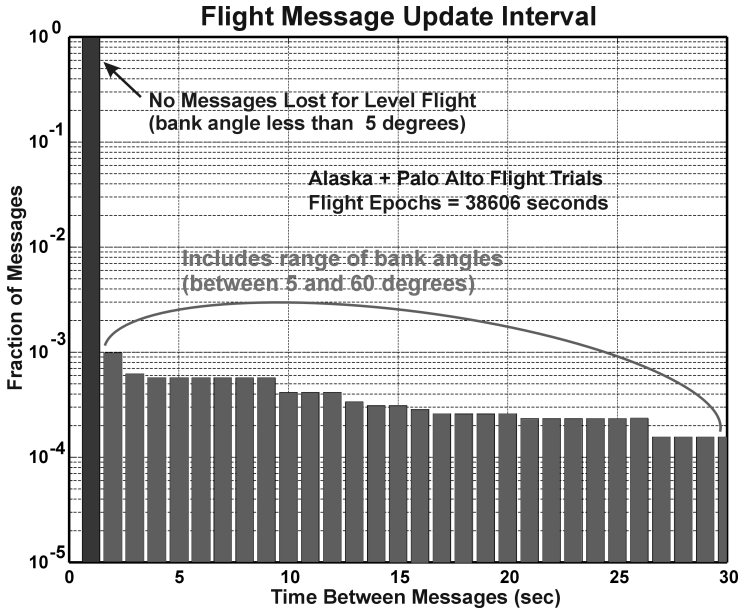

Figure 10: Message Loss Histogram. The Locally-Level Flight (< 5 degrees of bank) are All Contained in First Bar (Time Between Messages=1 sec)

The message stream was used to correct the position solution yielding availability results that were presented in [7, 13]. The flight tests were conducted under a variety of flight modes from precision approach to en-route. In an effort to stress the GEO link some of the flight maneuvers included 60 degree banks from side-to-side. Using data collected during the flight tests, it was possible to ascertain the message loss rate for the GEO satellite message stream.

The following sections overview the data loss observed in flight and develop a Markov model [16] for characterizing message losses in flight. This model is then used to characterize the availability of WAAS solutions across the U.S. using NSTB data.

IN-FLIGHT MESSAGE LOSS OBSERVATIONS

Flight tests were conducted in August 1998 in the region around Juneau, Alaska and on various dates from October to December 1998 in and around Palo Alto, California. These flight tests recorded the messages lost over time. Figure 10 shows the distribution of the spacing between the messages. As a single WAAS message is sent every second, the nominal spacing is also one second. All other durations indicate that a certain number of messages have been lost. The data in Figure 10 indicate messages lost in all modes of flight; including periods of steep banks (up to 60 degrees) for short periods to determine the robustness of the signal tracking and re-acquisition [13]. Even with these highly banked operations, the solution availability exceeded 98.5%. The data represents almost 11 hours of flight time (38644 one-second epoch). Figure 10 is the message loss histogram from the flight tests.

Using the symbol 0 to represent a received message, 1 to represent a lost message, and X to represent either a received or lost message, then the Figure 10 loss sequences can be written out. The bar to the farthest left (time between messages = 1) is the case for no losses, or 00. The next bar represents a single message loss, 01X, where the next message could be lost or received. The next bar (time between messages = 3) is the case for two sequential losses, 011X. The remaining sequences are 0111X, 01111X, 011111X, etc. These continue in this fashion up to 30 sequential losses.

As Figure 10 indicates, the overwhelming majority of the points fall into the bin which represents no loss (time difference between received messages = one second). All other outage durations are less probable than 4×10^{-3}. Of particular note is performanace during near level flight. *With a bank angle less than 5 degrees, there were no message losses*. This level-flight result was true in both Alaska and California flight operations where the locally-level elevations to the GEO satellite were different; 15 degrees for Alaska (POR) and 9 degrees for California (AOR-W). Figure 1 gives the elevation angles versus geographic location. This differs from the results presented previously where message loss occurred at 12 degrees of elevation. It may indicate that proper siting of an antenna on an aircraft can help defray some of the losses incurred by low elevation satellites. Additionally, the observed GEO satellite power level of the receiver-in-flight for all wings-level conditions (< 5 degrees of bank) always exceeded 40 dB-Hz and often exceeded 43 dB-Hz. This was true for both tracking GEO satellites AOR-W and POR in California as well as POR in Alaska

For those times when the aircraft was not level, the message loss occurred in groups or 'bursts.' Since all of the burst-losses occurred when the aircraft was not level, a strong correlation exists between message losses and aircraft orientation. Since the bank angle of the aircraft does not change instantly, message losses tend to persist and create message loss burst. This is important in extending the static reference receiver results from the previous sections to users in flight.

The following sections establish a Markov model for the flight message loss and extend them to multiple locations across the US using NSTB data.

MODEL OF FLIGHT MESSAGE LOSSES (BURST-MODE ERRORS)

Reference [14] described a simple Markov channel model that could be used for the characterization of message loss in the presence of atmospheric noise. This work was an extension of [15], which used partioned states to portray real communication channels. These methods suggested an approach that utilized a binary Markov chain to model the flight message losses. A brief introduction to random processes and Markov chains is given in [5, 15, 16].

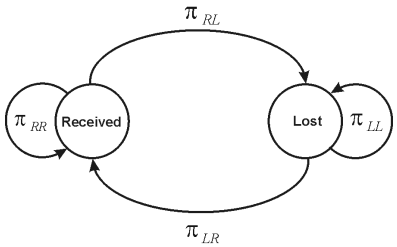

Figure 11: Burst Model Diagram

Figure 11 shows a transition probability diagram for a burst model which is a two-state Markov chain. The states are broken down into message received and message lost. This model is designed to capture the groups of messages lost. The transition probabilities are represented as described in [5, 16] by the transition probability matrix:

$$P = \begin{bmatrix} \pi_{RR} & \pi_{RL} \\ \pi_{LR} & \pi_{LL} \end{bmatrix} \tag{1}$$

where:

$$\begin{aligned} \pi_{RR} + \pi_{RL} &= 1 \\ \pi_{LR} + \pi_{LL} &= 1 \end{aligned} \tag{2}$$

Also known is the transition probability from the message-received state to message-lost, π_{RL}, which is simply the probability that a single message is lost. From inspection of Figure 10 this transition probability is on the order of 0.001, so for the Alaskan and California flight tests (including steep bank angles):

$$\pi_{RL} = 0.001 \tag{3}$$

To solve for the other model parameters, we apply Bayes' rule [6]:

$$P(A|B) = \frac{P(B|A)P(A)}{P(B)} \tag{4}$$

where $P(A|B)$ is the conditional probability of event A given event B, $P(B|A)$ is the conditional probability of event B given event A, $P(A)$ is the total probability of event A and $P(B)$ is the total probability of event B. Applying Bayes' rule to this model we have:

$$\pi_{LR} = \frac{\pi_{RL} P(R)}{P(L)} \tag{5}$$

where $P(R)$ is the total probability of a message being received and $P(L)$ is the total probability of a message being lost. For this data set the total probability of a message being lost was $P(L) = 0.0106$. The complementary total reception rate was

$$P(R) = 1 - P(L) = 0.9894 .$$

The full parameter set is solved by employing Equations (2), (3), (4) and (5) and the data in Figure 10:

$$\begin{aligned} P(L) &= 0.0106 \\ P(R) &= 1 - P(L) = 0.9894 \\ \pi_{RL} &= 0.0010 \\ \pi_{RR} &= 1 - \pi_{RL} = 0.9990 \\ \pi_{LR} &= \frac{\pi_{RL} \cdot P(R)}{P(L)} = \frac{0.001 \cdot 0.9894}{0.0106} = 0.0922 \\ \pi_{LL} &= 1 - \pi_{LR} = 0.9078 \end{aligned} \tag{6}$$

The function to generate the flight model loss is:

$$P_L(n) = \begin{cases} 1 - P(L) = P(R) & n = 0 \\ \pi_{RL} & n = 1 \\ \pi_{RL} \cdot (\pi_{LL})^{(n-1)} & n > 1 \end{cases} \tag{7}$$

where $P_L(n)$ represents the probability that *n* sequential messages are lost. Figure 12 is the comparison of the data to the model, $P_L(n)$, described in Equation (7).

These parameters form a good bound for short losses and slightly underestimate the longer losses as compared to actual losses. This forms a somewhat conservative estimate since part of the Alaska flight trials lowered the messaging performance by exercising very strong banking (60 degrees) during a period up to 15 minutes (900 seconds) in an alternating fashion. This high banking period represents less than 3% of the total flight data in Figures 10 and 12, so the influence is potentially large given the small overall percentages of loss. When the aircraft was operating at level or near-level flight (< 5 degrees), there were no recorded message losses. This near-level flight profile most closely represents approach to landing where the aircraft is less than 5 miles from touchdown.

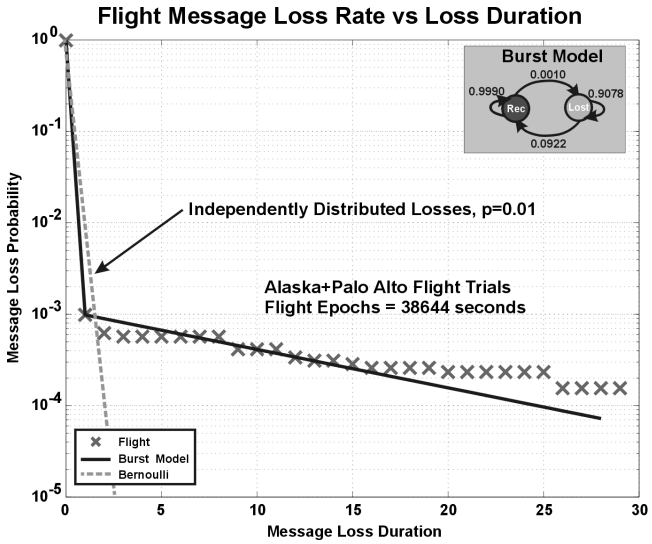

Figure 12: Flight Message Loss Compared to Burst Model Realization (3% of Data Including 60 Degree Bank Angles)

The dashed line in Figure 12 represents independently distributed losses. The independent losses were treated as a Bernoulli distribution (see the next section) with a total probability of message loss, p=0.01. The burst model performs much better in comparison to independently distributed message losses in terms of its correspondence to the flight data.

With a model for the flight message losses, the effects on integrity and availability can be established. The following section looks at the influence of the burst loss model on the overall integrity of the WAAS message signal compared to the assumption that the losses are independently distributed.

BURST LOSS EFFECT ON INTEGRITY

As stated in the previous section, the assumption is that three repeats are used for critical alarm messages or changes in the correction bounds (UDRE, GIVE). With independent message losses and a specification for those individual losses set at 0.001, the integrity level of 10^{-8} is achieved ($\left(10^{-3}\cdot 10^{-3}\cdot 10^{-3}=10^{-9}\right)<10^{-8}$).

However, the preceding sections have shown that flight message losses are not independent. In order to determine the integrity of the alarm message for the burst model, the probability distribution from Equation (7) was used to estimate the probability that three successive messages are lost. By fixing the value of $\pi_{RL}=0.001$, the total probability of message loss, *P(L)*, was adjusted between loss rates of 10^{-4} and 10^{-1} and new model parameters were determined from Equations (2), (3), (4) and (5) and used in Equation (6) to develop the second line in Figure 13. The dotted line in Figure 13 represents the probability that three independent message losses have occurred.

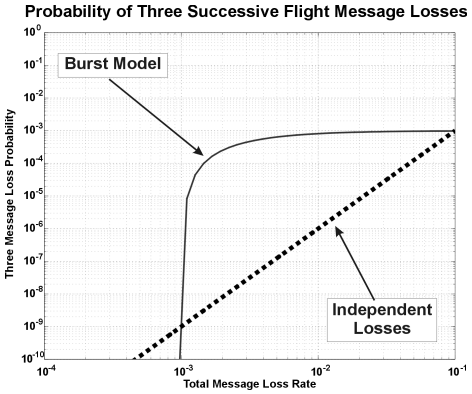

Figure 13: Comparison of Burst Model and Independent Loss Assumptions on the Probability that Three Successive Messages are Lost

The total message loss rate must be less than 1.01×10^{-3} using the burst model to meet the requirement that the probability of loss of three successive messages is less than 10^{-8}. This is very close to the requirement set forth in the MOPS [1] where independent losses were assumed at a 1×10^{-3} loss rate. However, the burst model has a very high slope near the critical message loss rate due mainly to the value of $\pi_{RL}=0.001$. Slightly higher or lower losses could dramatically impact this result. Additionally, different values of π_{RL} have a strong effect on the results. The results from a previous section, Figure 4, suggest that message loss rates at least an order of magnitude better than 1.01×10^{-3} can be achieved if the power level for the receiver exceeds 36 dB-Hz. Significant margin in the message loss rate may even be attained even at 34 dB-Hz.

With a highly conservative flight message loss burst model in hand, the flight test values can be extended to multiple fixed sites across the US to assess the availability of the WAAS solution under general flight conditions.

MESSAGE LOSS IMPACT ON AVAILABILITY

The following two sections look at the availability of WAAS solutions for four sites across the US utilizing the burst message loss model developed in the previous section. The data was processed by the Stanford TMS program using data from the NSTB with models implemented to simulate message loss. The first section will assume a random message loss, with each loss uncorrelated to the others. It is important to note that each of the stations used in this study was set as passive, i.e., the station in question was *not* used in the formulation of the correction message. The independent loss results serve as the reference for burst message losses on availability.

INFLUENCE OF RANDOM MESSAGE LOSS

The Stanford TMS software was modified to simulate random message losses. The loss model was simulated as a Bernoulli distribution [5]. A Bernoulli distribution is a two-state version of the binomial random variable [6]. The probability mass function (pmf) of a Bernoulli random variable, *X*, is defined by:

$$p_X(k) = P(X = k) = p^k (1-p)^{1-k} \qquad k = 0,1 \quad (8a)$$

where $0 \le p \le 1$. The cumulative distribution function (cdf), $F_X(x)$, of the Bernoulli random variable, *X*, is given by:

$$F_X(x) = \begin{cases} 0 & x < 0 \\ 1-p & 0 \le x \le 1 \\ 1 & x > 1 \end{cases} \qquad (8b)$$

Figure 14 shows the distribution of the VAL=20 meter availability from four stations in the NSTB network. The influence of the random, independently distributed message loss is non-existent for loss rates less than 10^{-3} and there are no significant increases for less than a rate 10^{-2}. This validates the assumption in the specification that independently distributed message losses in combination with a loss rate less than 10^{-3}, do not affect the availability.

Of particular note is that the Sitka Alaska station does not meet 10^{-3} availability even with zero message loss. The extreme northern location of Sitka, Alaska limits the visibility of the GPS satellites (see Figure 1.7) and, therefore, severely limits navigation solution availability. Comp presented results showing that the availability of a GEO ranging signal could, in a specific case, improve the overall availability of the solution in Southeastern Alaska (i.e., the Juneau and Sitka area) [13].

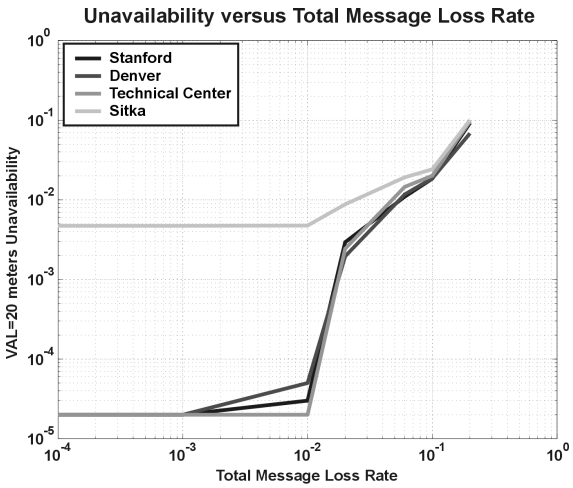

Figure 14: WAAS Correction Unavailability for Independently Distributed Message Loss at Four NSTB Locations (Bernoulli Random Variable)

The following section shows the impact of applying the burst model to the availability of the WAAS solution.

BURST LOSS EFFECT ON AVAILABILITY

The previous results indicated that there were only subtle effects in availability under 10^{-2} message loss rates. The parameters are modified for various total probability message loss rates, $P(L)$. As noted to in the previous section, the flight data had a total message loss probability of $P(L) = 0.0106$. This value, along with the transition probability in Equation (3), allowed the computation of all transition probabilities within the burst model by using Equations (2) and (5). By selecting different total probabilities of message loss, a higher or lower loss rate can be extrapolated from the same burst model. The transition probability in Equation (3) remained fixed in all cases. The total message loss probabilities tested were:

$$P(L) = \begin{cases} 0.0005 \\ 0.0010 \\ 0.0050 \\ 0.0106 \quad \leftarrow \text{flight result} \\ 0.0500 \end{cases} \qquad (9)$$

Each of the total probabilities in Equation (9) was used to determine the burst model parameters subject to Equation (3). To calculate each of the transition probabilities:

$$\begin{aligned} \pi_{RR} &= 0.9990 \\ \pi_{RL} &= 0.0010 \\ \pi_{LR} &= \frac{\pi_{RL} * P(L)}{P(R)} = \frac{0.0010 * P(L)}{1 - P(L)} \\ \pi_{LL} &= 1 - \pi_{LR} \end{aligned} \qquad (10)$$

The formulation in Equation (10) allows for the extension of the burst model along the horizontal axis shown in Figure 14 since that axis represents the total message loss

rate. By constraining the solution to Equation (3), the transition probability from the 'received' state to the 'lost' state remains fixed. This causes the length of the outages to increase to accommodate the larger total loss probability. The 'tail' in Figure (12) is flattened as the total loss probability increases.
The message losses were simulated according to this burst model and processed with the TMS program using the NSTB data. This is the same data set used to generate Figure 14.

Figure 15 shows the results of the burst model on the WAAS solution availability for the various total message loss probabilities given in Equations (9) and (10). The horizontal axis represents the equivalent total message loss rate or *P(L)* from Equation (10). This shows that for three of the four stations, the impact on availability even at the lowest loss rates has been degraded by an order of magnitude. While the performance of the burst model message losses are significantly worse than with the independent loss assumption, the performance still meets 99.9% availability when the total message losses exceed 0.5%. As in Figure 14, in Figure 15 the station at Sitka stands out. In this case, the burst model has a smaller relative influence on the performance in comparison to the other stations. This indicates that when the initial performance of a station (or an aviation user) is poor, then the influence of burst mode losses is less than when performance is initially good. When the loss rates approaches 10^{-2}, the performance at all stations are nearly identical.

The large circles on the plot indicate the flight modes when the bank angles were small. This small bank-angle case corresponded to no message losses and hence the nominal performance at each of the reference stations. Three stations, Stanford, Denver and the Technical Center are represented by the lower circle and Sitka is represented by the upper circle for no message loss.
As noted previously, these small bank angle cases model the critical approach phases of flight. Therefore, it may be deduced from this data that message loss performance for the aircraft on approach can be approximated by the stationary reference station availability profile and the burst model developed herein.

Of the total number of messages, roughly 3% represent a period when the aircraft was maneuvering in 60-degree banks back-and-forth. These maneuvers have a strong influence on the total message losses and make these results very conservative for estimating the availability of WAAS solutions during precision approaches. When preparing for final approach, bank angles are either kept small or range from 20-30 degrees for very short periods of time.

These results show that the MOPS specification [1] *for availability in a precision approach mode has been achieved even with a highly conservative model for flight message loss.*

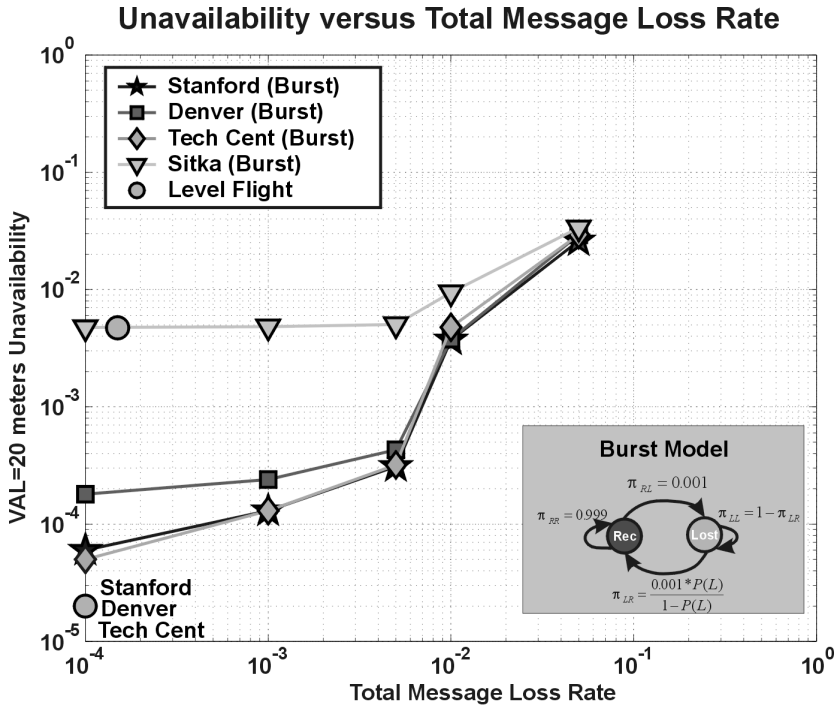

Figure 15: WAAS Correction Unavailability Versus Burst Model Equivalent Total Message Loss Rate at Four NSTB Locations

ACKNOWLEDGEMENTS
This work was supported by the Federal Aviation Administration under Grant 95-G-005. The authors gratefully acknowledge Barbara Lingberg, Steve Kalinowski, Jean-Christophe Geffard, Dan Hanlon and Dave Peterson for their work with and for the NSTB that was critical in the completion of this undertaking. We would also like to thank Tom Darter of COMSAT for his careful attention during GEO communication operations and Bruce Gribble of Stanford Telecommunications for his assistance studying receiver characteristics. In addition the authors would also like to extend thanks to Sky and Kevin McCoy of Sky Research who carried out the piloting work during these tests. And finally we would like to thank all of the members of the Stanford GPS Laboratory for their continuing effort especially, Demoz Gebre-Egziabher, Roger Hayward, Andy Barrows, Andrew Hansen, Chad Jennings and Doug Archdeacon.

RERERENCES

[1] "Minimum Operational Performance Standards for Global Positioning System/Wide Area Augmentation System Airborne Equipment," RTCA Document No. RTCA/DO-229A, June 1998, prepared by RTCA SC-159

[2] Benedicto, J., Michael, P., Ventura-Traveset, J., "EGNOS, the European Regional Augmentation to GPS and GLONASS," Proceedings of the fifth ESA International Workshop on DSP Techniques Applied to Space Communications, Noorwijk, The Netherlands, 23-25 September 1998

[3] Ventura-Traveset, J., *et al*., "A technical review of SBAS interoperability issues from the EGNOS perspective," Proceedings of 2nd European Symposium of Global Navigation Satellite Systems (GNSS98), Toulouse, France, 20-23 October 1998

[4] Satellite-Based Augmentation System (SBAS) Standards and Recommended Practices (SARPS), Draft 7, Aug. 1998, International Civil Aviation Organization (ICAO)

[5] Hsu, H.P., *Probability, Random Variables, & Random Processes*, McGraw-Hill, New York, 1997

[6] Leon-Garcia, A*., Probability and Random Processes for Electrical Engineers*, 2nd Edition, Addison Wesley, 19970

[7] Fuller, R.A., Walter, T., Houck, S., and Enge, P., "Flight Trials of a Geostationary Satellite Based Augmentation System at High Latitudes and for Dual Satellite Coverage," Proceedings of the Institute of Navigation 1999 National Technical Meeting, January, 1999

[8] Schnaufer, B.A., McGraw, G.A., "WAAS Receiver Carrier Tracking Loop and Data Demodulation Performance in the Presence of Wideband Interference," *Navigation: Journal of the Institute of Navigation*, Vol. 44, No. 1, Spring 1997

[9] Enge, P., "WAAS Messaging System: Data Rate, Capacity, and Forward Error Correction," *Navigation: Journal of the Institute of Navigation*, Vol. 44, No. 1, Spring 1997

[10] Hegarty, C.J., "Analytical Derivation of Maximum Tolerable In-Band Interference Levels for Aviation Applications of GNSS," *Selected Papers on the Wide-Area Augmentation System: Volume VI*, The Institute of Navigation, 1999

[11] Hayward, R.C., Powell, J.D., "Real Time Calibration of Antenna Phase Errors for Ultra Short Baseline Attitude Systems," Proceedings of the ION GPS 98, The Institute of Navigation, September 1998

[12] Alter, K.W., Barrows, A.K., Enge, P.K., Jennings, C.W., Parkinson, B.D., Powell, J.D., "In-flight Demonstrations of Curved Approaches and Missed Approaches in Mountainous Terrain," Proceedings of the ION GPS 98, The Institute of Navigation, September 1998

[13] Comp, C., Walter, T., Fuller, R., Barrows, A., Alter, K., Gebre, D., Hayard, R., Jennings, C., Hansen, A., Phelts, R.E., Archdeacon, D., Enge, P., Powell, J.D., Parkinson, B., "Demonstration of WAAS Approach and Landing in Alaska," Proceedings of ION GPS 98, The Institute of Navigation, September 1998

[14] Olson, K.E., Enge, P.K., "Forward Error Correction for an Atmospheric Noise Channel," IEEE Transactions on Communications, Vol. 40, No. 5, May 1992

[15] Fritchman, B.D., "A Binary Channel Characterization Using Partitioned Markov Chains," IEEE Transactions on Information Theory, Vol. IT-13, No. 2, April 1967

[16] Fuller, R.A*., Aviation Utilization of Geostationary Satellites for the Augmentation to GPS: Ranging and Datalink*, Department of Aeronautics and Astronautics Thesis, Stanford University, 2000